E2EDiff: Direct Mapping from Noise to Data for Enhanced Diffusion Models

Zhiyu Tan[1,2]*, WenXu Qian[1,2]*, Hesen Chen[2], Mengping Yang, Lei Chen[1,2], Hao Li[1,2]†

[1] Fudan University   [2] Shanghai Academy of Artificial Intelligence for Science

Abstract

Diffusion models have emerged as a powerful framework for generative modeling, achieving state-of-the-art performance across various tasks. However, they face several inherent limitations, including a training-sampling gap, information leakage in the progressive noising process, and the inability to incorporate advanced loss functions like perceptual and adversarial losses during training. To address these challenges, we propose an innovative end-to-end training framework that aligns the training and sampling processes by directly optimizing the final reconstruction output. Our method eliminates the training-sampling gap, mitigates information leakage by treating the training process as a direct mapping from pure noise to the target data distribution, and enables the integration of perceptual and adversarial losses into the objective. Extensive experiments on benchmarks such as COCO30K and HW30K demonstrate that our approach consistently outperforms traditional diffusion models, achieving superior results in terms of Fréchet Inception Distance (FID) and CLIP score, even with reduced sampling steps. These findings highlight the potential of end-to-end training to advance diffusion-based generative models toward more robust and efficient solutions.

1. Introduction

Generative models have emerged as a cornerstone of modern machine learning, providing a robust framework for synthesizing complex data distributions. Early breakthroughs in this domain include Variational Autoencoders (VAEs)[6], which leverage probabilistic latent variable models to learn structured representations of data and facilitate generation. Generative Adversarial Networks (GANs)[3] followed, introducing adversarial training strategies that enabled the generation of high-quality and realistic samples. Recently, diffusion models have gained prominence as a cutting-edge generative approach, utilizing iterative denoising processes to achieve remarkable fidelity

---

*Equal contribution.
†Corresponding author.

and diversity in their outputs [5]. Concurrently, consistency models[17] have attracted attention for their capacity to align intermediate representations throughout the generation process, enabling faster sampling with enhanced stability and reliability. These advancements underscore the ongoing trade-offs between model quality, sampling efficiency, and consistency in the field of generative modeling.

Among generative modeling approaches, diffusion models have achieved remarkable success across various tasks, establishing state-of-the-art performance [5, 18]. However, despite their impressive achievements, diffusion models face several inherent limitations. These challenges can be categorized into three primary issues: **1.Training-Sampling Gap:** Diffusion models suffer from a fundamental mismatch between their training and testing processes. During training, the model is optimized to predict noise in a single-step denoising task for randomly sampled time steps. In contrast, the testing phase involves a multi-step iterative denoising process. This discrepancy prevents the model from effectively capturing and mitigating the compounded errors that arise during sampling, especially when fewer sampling steps are used. Consequently, the training objectives fail to align well with testing conditions, limiting both the efficiency and robustness of the generative process. **2.Information Leakage in x_T:** A critical issue emerges from the progressive noising process used in training. Ideally, the final noised state x_T should approximate pure Gaussian noise to ensure consistency with the theoretical assumptions of the reverse denoising process [5]. However, due to minor inconsistencies in the forward process, x_T often deviates from true Gaussian noise, leading to information leakage. This deviation compromises the model's ability to accurately reconstruct data, introducing biases that degrade the quality of the generated outputs. **3.Limited Loss Function Flexibility:** The training paradigm of diffusion models, which involves random sampling of intermediate steps, poses challenges for incorporating advanced loss functions, such as perceptual loss or GAN loss, directly on intermediate outputs. It is widely recognized that training with GAN loss can effectively enhance the detail richness of generated images, making them appear more realistic. These loss functions are crucial for improving the percep-

tual quality and semantic coherence of generated results. However, the inherent structure of diffusion models limits their ability to fully leverage such loss functions, thereby restricting their potential to achieve superior visual fidelity and high-quality synthesis, particularly for tasks requiring fine-grained detail generation. Collectively, these limitations hinder the performance, consistency, and flexibility of diffusion models, highlighting the necessity for innovations that address these challenges while maintaining their generative strengths.

To address these limitations, we propose an end-to-end training framework for diffusion models that aligns the training and sampling processes while addressing key challenges. Unlike traditional methods that focus on noise prediction at randomly sampled intermediate steps, our approach directly optimizes the final reconstruction, transforming pure Gaussian noise into the target distribution through a unified process. This design bridges the training-sampling gap by enabling the model to learn to handle compounded errors across all sampling steps. Additionally, it eliminates information leakage in x_T by treating the training process as a direct mapping from pure noise to the data distribution. The unified objective also supports the integration of perceptual and adversarial losses, enhancing the fidelity and semantic consistency of generated outputs while maintaining theoretical consistency and robustness.

Extensive experiments conducted on widely recognized benchmarks, such as COCO30K[8] and HW30K[2], validate the effectiveness of our proposed approach. Our method consistently surpasses existing state-of-the-art diffusion models across critical performance metrics, including Fréchet Inception Distance (FID)[4] and CLIP score[12], while demonstrating strong performance and advantages with fewer sampling steps. These findings underscore the transformative potential of end-to-end training in advancing diffusion-based generative models. By directly addressing the core limitations of existing approaches, our framework sets a new standard for efficiency, quality, and consistency in generative modeling.

2. Related Work

2.1. Generative models.

Generative models have undergone significant evolution, starting from Variational Autoencoders (VAEs)[6] and Generative Adversarial Networks (GANs)[3]. VAEs leverage probabilistic latent variable models to generate structured data but often struggle with producing high-fidelity samples due to their reliance on explicit likelihood optimization. GANs, on the other hand, use adversarial training to synthesize visually appealing data but are prone to instability and mode collapse, limiting their scalability. Modern advancements, such as diffusion models and latent gener-

ative approaches, have addressed some of these issues by introducing iterative refinement and efficient latent representations. However, these methods often involve complex training dynamics and lack alignment between training and inference phases[5, 15, 13]. Unlike these methods, our end-to-end approach directly optimizes the generative trajectory, ensuring consistency between training and sampling while reducing complexity.

2.2. Diffusion Models

Diffusion models, such as Denoising Diffusion Probabilistic Models (DDPM) [5] and their extensions like stochastic differential equations (SDE) [18] and ordinary differential equations (ODE), have set the benchmark for generative modeling across various tasks. These models operate by progressively transforming Gaussian noise into the target data distribution through a multi-step denoising process, leveraging a learned sequence of reverse transformations. Despite their remarkable success, diffusion models face a significant limitation stemming from a fundamental training-sampling mismatch. During training, the model is optimized to predict noise in a single-step denoising task for randomly sampled time steps. However, in the sampling phase, the model must iteratively refine the data across multiple steps [15]. This discrepancy introduces a training-sampling gap, leading to compounded errors and inefficiencies during inference. Our proposed method addresses these limitations by unifying the training and sampling processes through an end-to-end optimization framework. Instead of focusing on intermediate noise predictions, we directly optimize the final reconstruction, aligning the model's training objectives with the sampling procedure. This approach not only bridges the training-sampling gap but also mitigates error accumulation and enhances inference efficiency. By directly targeting the quality of the generated outputs, our method achieves superior performance, paving the way for more robust diffusion-based generative models.

2.3. Accelerating DMs.

Efforts to accelerate diffusion models have introduced several innovative techniques. Latent diffusion models (LDM)[13] reduce computation by operating in a compressed latent space, while progressive distillation minimizes the number of sampling steps through staged knowledge transfer[14, 7]. Consistency models align intermediate representations to facilitate fast sampling[17, 16], and latent consistency models extend this concept to latent spaces for further efficiency gains[10]. However, these approaches often involve additional assumptions, such as specific network architectures or auxiliary losses, and may still rely on multi-step sampling procedures. Our method simplifies the generative process by learning the entire trajectory in an end-to-end manner, eliminating reliance on step-wise refinements

and achieving robust performance with fewer constraints.

3. Method

3.1. Background

The Diffusion Model[5] serves as the foundational framework. It defines a forward process that progressively adds Gaussian noise to data samples $\mathbf{x}_0 \sim q(\mathbf{x}_0)$ over T time steps, modeled as:

$$q(\mathbf{x}_t|\mathbf{x}_{t-1}) = \mathcal{N}(\mathbf{x}_t; \sqrt{1 - \beta_t}\mathbf{x}_{t-1}, \beta_t\mathbf{I}), \qquad (1)$$

where $\beta_t \in (0, 1)$ are noise variance schedules. The reverse process, which aims to reconstruct clean data, is parameterized as:

$$p_\theta(\mathbf{x}_{t-1}|\mathbf{x}_t) = \mathcal{N}(\mathbf{x}_{t-1}; \mu_\theta(\mathbf{x}_t, t), \Sigma_\theta(\mathbf{x}_t, t)). \quad (2)$$

During training, the model learns to predict the noise ϵ added to the data $\mathbf{x}_t$ at each time step by optimizing the objective:

$$L(\theta) = \mathbb{E}_{q(\mathbf{x}_0,\mathbf{x}_t,\epsilon)}\left[\|\epsilon - \epsilon_\theta(\mathbf{x}_t, t)\|^2\right]. \qquad (3)$$

Crucially, this loss function optimizes the model for a single denoising step, assuming independence between steps. However, during sampling, the model performs multi-step denoising, where each step depends on the accuracy of the preceding steps, creating a coupling between time steps. This mismatch between single-step training and multi-step sampling often limits the quality of the generated samples, as errors can accumulate across steps.

The **Latent Diffusion Model (LDM)**[13] addresses the computational inefficiency of operating in the high-dimensional data space by introducing a latent representation $\mathbf{z}_0 = \mathcal{E}(\mathbf{x}_0)$, obtained via an encoder $\mathcal{E}$. The forward and reverse diffusion processes are then performed in the latent space:

$$q(\mathbf{z}_t|\mathbf{z}_{t-1}) = \mathcal{N}(\mathbf{z}_t; \sqrt{1 - \beta_t}\mathbf{z}_{t-1}, \beta_t\mathbf{I}), \qquad (4)$$

$$p_\theta(\mathbf{z}_{t-1}|\mathbf{z}_t) = \mathcal{N}(\mathbf{z}_{t-1}; \mu_\theta(\mathbf{z}_t, t), \Sigma_\theta(\mathbf{z}_t, t)). \qquad (5)$$

The training objective remains similar:

$$L(\theta) = \mathbb{E}_{q(\mathbf{z}_0,\mathbf{z}_t,\epsilon)}\left[\|\epsilon - \epsilon_\theta(\mathbf{z}_t, t)\|^2\right]. \qquad (6)$$

While LDM reduces computational costs by operating in a lower-dimensional space, it inherits the same limitation as diffusion models: the training is optimized for a single denoising step, while the sampling process involves multi-step refinement, where errors can propagate and degrade the final result.

3.2. E2EDiff

To address the aforementioned limitations of diffusion models, particularly the mismatch between single-step training and multi-step sampling, we propose an **end-to-end training approach** that directly optimizes the generation process from pure Gaussian noise $\mathbf{z}_T$ to the reconstructed latent representation $\mathbf{z}_0$, conditioned on textual descriptions. This approach simplifies the training objective and enables joint optimization over the entire sampling trajectory in the latent space, effectively aligning training and sampling objectives.

In traditional diffusion models, the training objective distributes the loss across all T timesteps, with the model trained to predict the noise ϵ added at each intermediate timestep $\mathbf{z}_t$. This involves T separate losses during training, while the final generative performance is indirectly affected by the coupling of intermediate timesteps during sampling. In contrast, our method focuses on the ultimate reconstruction quality of $\mathbf{z}_0$ by training the model end-to-end with a single loss. Specifically, we redefine the training objective by applying the loss directly to the reconstructed latent result $\hat{\mathbf{z}}_0$, as follows:

$$L_{\text{recon}}(\theta) = \mathbb{E}_{q(\mathbf{z}_T,\mathbf{z}_0)}\left[d(\mathbf{z}_0, \hat{\mathbf{z}}_0)\right], \qquad (7)$$

where $\hat{\mathbf{z}}_0$ is the output of the generative process starting from pure Gaussian noise $\mathbf{z}T$ and conditioned on the text embedding. The metric function $d(\cdot, \cdot)$ quantifies the distance between the ground truth latent representation $\mathbf{z}_0$ and the reconstructed output $\hat{\mathbf{z}}_0$. By operating in the latent space instead of the pixel space, our approach leverages pre-trained image encoders for efficient and semantically meaningful representations.

The training process, outlined in Algorithm 1, involves learning a mapping from a noisy latent input $\mathbf{z}_T$ to the clean latent representation $\mathbf{z}_0$, conditioned on a textual embedding $\mathbf{e_c}$ obtained from a pre-trained text encoder. To ensure stability and improve model performance, Exponential Moving Average (EMA) is employed to update the model parameters incrementally.

A critical aspect of training lies in defining the metric function $d(\cdot, \cdot)$, which measures the similarity between the predicted latent representation $\hat{\mathbf{z}}_0$ and the target $\mathbf{z}_0$. Several choices are commonly used, depending on the specific goals of the task. The **L1 Loss**, defined as $d_{\text{L1}}(\mathbf{z}_0, \hat{\mathbf{z}}_0) = \|\mathbf{z}_0 - \hat{\mathbf{z}}_0\|_1$, calculates the mean absolute error (MAE) and is known for its robustness to outliers. In contrast, the **L2 Loss**, $d_{\text{L2}}(\mathbf{z}_0, \hat{\mathbf{z}}_0) = \|\mathbf{z}_0 - \hat{\mathbf{z}}_0\|_2^2$, computes the mean squared error (MSE), which penalizes larger deviations more strongly, potentially improving convergence but being more sensitive to outliers. Another widely used metric is the **Learned Perceptual Image Patch Similarity (LPIPS) Loss**, expressed as $d_{\text{LPIPS}}(\mathbf{z}_0, \hat{\mathbf{z}}_0) = \text{LPIPS}(\mathbf{z}_0, \hat{\mathbf{z}}_0)$. This loss leverages features from pre-trained neural networks to
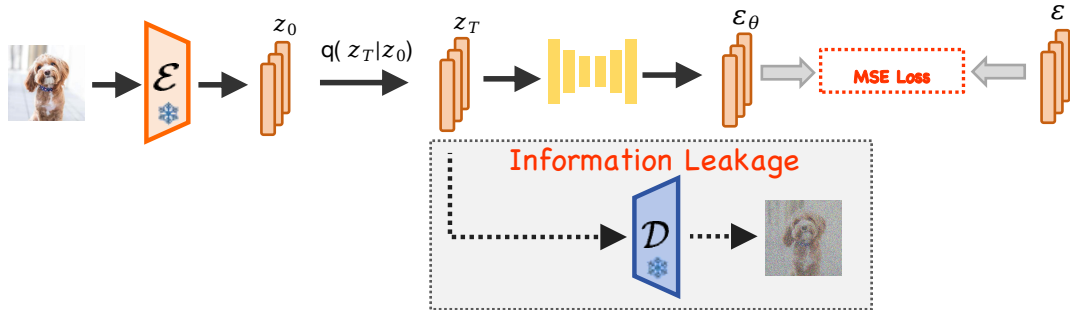
(a) Single-step Training
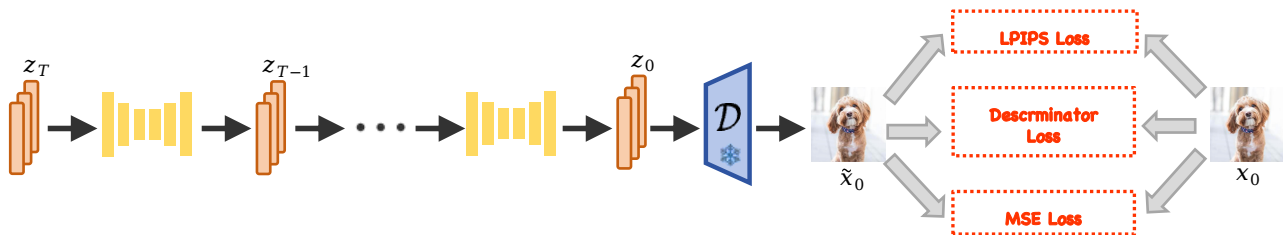
(b) End-to-end Training

Figure 1. **Comparison of two training methods for diffusion models.** (a) illustrates the **single-step training method**, where the model is trained to predict noise in a single denoising step for randomly sampled time steps. This approach introduces a training-sampling gap, as the training focuses on single-step denoising, whereas testing requires iterative multi-step denoising. Furthermore, the forward noising process can result in information leakage, where the final state x_T deviates from ideal Gaussian noise, compromising the reconstruction quality. (b) illustrates the **end-to-end training method**, which directly optimizes the entire sampling trajectory. Beginning with pure Gaussian noise, the model generates images through multi-step sampling, aligning the training and testing processes seamlessly. This approach effectively eliminates information leakage and enables the integration of advanced loss functions, such as perceptual and GAN losses, thereby improving the fidelity, semantic consistency, and overall quality of the generated images.

better align with human perceptual judgments of visual similarity, making it particularly effective in improving output quality for image-generation tasks. Additionally, a **hybrid metric** can be employed to combine these approaches, with a weighted formulation $d(\mathbf{z}_0, \hat{\mathbf{z}}_0) = \lambda_{\text{L1}} d_{\text{L1}} + \lambda_{\text{L2}} d_{\text{L2}} + \lambda_{\text{LPIPS}} d_{\text{LPIPS}}$, where weights $\lambda_{\text{L1}}, \lambda_{\text{L2}}, \lambda_{\text{LPIPS}}$ balance their contributions, enabling the model to leverage the complementary strengths of these loss functions.

The training process involves sampling a random timestep $t \sim \{1, \dots, T\}$ during each training iteration to construct noisy samples $\mathbf{z}_t$. Instead of training the model step-by-step with individual losses at each timestep, our approach applies the reconstruction loss exclusively to the final output $\hat{\mathbf{z}}_0$, ensuring end-to-end optimization over the entire generation trajectory. This method aligns the training objective with the sampling procedure, mitigating the error propagation issues present in conventional diffusion models. Furthermore, the flexibility of the reconstruction loss L_{recon} to incorporate various metric functions $d(\cdot, \cdot)$ allows for a diverse range of objectives. For example, perceptual quality can be prioritized by adding LPIPS loss, while structural accuracy can be enhanced with L1 or L2 loss. These

choices and their effects are extensively evaluated in the experimental section of this paper.

An additional advantage of this approach is its flexibility to incorporate auxiliary objectives, such as adversarial training. By introducing a GAN-based loss L_{GAN}, the model can further improve the perceptual quality of the generated data. The combined training objective becomes:

$$L_{\text{total}}(\theta) = L_{\text{recon}}(\theta) + \lambda_{\text{GAN}} L_{\text{GAN}}(\theta), \quad (8)$$

where λ_{GAN} controls the weight of the adversarial loss. The reconstruction loss ensures faithful reproduction of the data, while the adversarial loss encourages high-quality and realistic outputs. This approach addresses the core limitations of existing diffusion models, providing a unified and flexible framework for efficient and high-quality generation.

4. Experiment

4.1. Experimental Setting

4.1.1 Datasets

To enhance the aesthetic quality and semantic consistency of the dataset, we began by integrating the COYO dataset[1]

4

Algorithm 1: End-to-End Training in Latent Space for Text-to-Image Diffusion with EMA

Input: θ: Model parameters; θ_{EMA}: EMA model parameters; τ: EMA decay rate; T: Number of diffusion steps; $d(\cdot, \cdot)$: Reconstruction loss metric; $\mathcal{D}$: Paired image-caption training dataset $\{(\mathbf{x}_0, \mathbf{c})\}$; α_t, σ_t: Noise schedule parameters; θ_{pre}: Pre-trained model parameters.

Output: Optimized model parameters θ^* and EMA parameters θ_{EMA}^*.

1 **Initialize:** $\theta \leftarrow \theta_{\text{pre}}$ and $\theta_{\text{EMA}} \leftarrow \theta$.

2 **while** *not converged* **do**

3   Sample $(\mathbf{x}_0, \mathbf{c}) \sim \mathcal{D}$;

4   Encode $\mathbf{x}_0$ to latent space: $\mathbf{z}_0 = E(\mathbf{x}_0)$;

5   Encode caption $\mathbf{c}$: $\mathbf{e_c} = T(\mathbf{c})$;

6   Sample initial noise: $\mathbf{z}_T \sim \mathcal{N}(\mathbf{0}, \mathbf{I})$;

7   **for** $t = T$ *to* 1 **do**

8   Sample $\mathbf{z} \sim \mathcal{N}(\mathbf{0}, \mathbf{I})$;

9   Compute $\hat{\mathbf{z}}_t \leftarrow \mathbf{z}_t + \sqrt{\alpha_t^2 - \sigma_t^2} \cdot \mathbf{z}$;

10   Predict the denoised latent:
          $\mathbf{z}_t \leftarrow G_\theta(\hat{\mathbf{z}}_t, \mathbf{e_c}, t)$;

11   **end**

12   Set $\hat{\mathbf{z}}_0 = \mathbf{z}_{t=0}$ (final predicted latent variable);

13   Compute reconstruction loss:
       $L_{\text{recon}} = d(\mathbf{z}_0, \hat{\mathbf{z}}_0)$;

14   Backpropagate and update θ:
       $\theta \leftarrow \theta - \eta \nabla_\theta L_{\text{recon}}$;

15   Update EMA parameters:
       $\theta_{\text{EMA}} \leftarrow \text{stopgrad}(\tau \theta_{\text{EMA}} + (1 - \tau)\theta)$;

16 **end**

17 **Return:** Optimized model parameters θ^* and EMA parameters θ_{EMA}^*

---

with an internally curated collection and conducting rigorous screening. Only images with aesthetic scores exceeding 5.5 were retained, ensuring superior visual quality. To generate captions, we employed the LLaVA 13B model[9], which leverages robust language understanding and image description generation capabilities to produce highly accurate and semantically consistent captions automatically. After filtering and captioning, we selected 120k high-quality images to form our final training dataset.

4.1.2 Baselines

To evaluate the performance of our approach, we conducted comparisons with several state-of-the-art text-to-image generation models, including SDXL [11], SDXL-Turbo, SDXL-Lightning [7], Latent Consistency Model (LCM) [10], and PixArt-δ [2]. SDXL is a large-scale diffusion model renowned for producing high-quality images at a resolution of 1024×1024, while SDXL-Turbo and SDXL-Lightning are optimized variants designed to accelerate inference by reducing sampling steps without sacrificing visual quality, making them practical for real-time applications. PixArt-δ leverages Latent Consistency Modeling (LCM), enabling efficient image generation in just four sampling steps through a lightweight architecture and pre-trained components, effectively balancing computational efficiency and output fidelity. Similarly, LCM focuses on reducing the computational complexity of the generation process, offering an appealing solution for resource-constrained scenarios. These comparisons underscore the diverse trade-offs in contemporary approaches between efficiency, scalability, and image quality, against which our method demonstrates significant competitive advantages.

4.1.3 Evaluation Metrics

To validate the effectiveness of our approach, we employed three metrics to assess the quality of generated images and their alignment with textual descriptions: FID on COCO30k, FID on Huawei30k, and CLIP score. FID evaluates the distributional similarity between real and generated data, with separate assessments on the COCO30k and Huawei30k datasets. The CLIP score measures the semantic correspondence between images and their associated captions. For fair comparisons, we followed the evaluation methodology introduced in PixArt-δ [2]. Specifically, FID evaluations were conducted on Huawei30k, a dataset introduced in PixArt-δ, containing 30k high-quality text-image pairs with remarkable aesthetic value and precise semantic annotations. Additional evaluations on the widely used COCO30k dataset provided consistent benchmarking against existing generative models. These metrics collectively highlight the superior perceptual quality and semantic alignment achieved by our approach.

4.1.4 Implementation Details

Our model was initialized using the pretrained PixArt-δ model[2] to leverage its robust text-to-image generation capabilities. The training process was carried out on 64 NVIDIA A100 GPUs, utilizing a batch size of 8 and a total of 24k training steps. We adopted the AdamW optimizer, configured with a weight decay of 1×10^{-8} and a fixed learning rate of 1×10^{-6}, ensuring effective gradient updates while mitigating overfitting. To maintain stable and smooth updates of model weights, an Exponential Moving Average (EMA) with a decay coefficient of 0.95 was employed throughout the training process. The experiments were conducted on an internal dataset comprising 120k high-quality images, specifically curated to cover a diverse range of subjects and styles, providing a robust foun-

dation for training. This setup enabled our model to achieve consistent performance improvements across all evaluation metrics.

4.2. Main Results

Table 1. Quantitative comparison of our method with state-of-the-art approaches on text-to-image synthesis tasks at 1024×1024 resolution. This table compares various methods based on COCO FID, HW FID, and CLIP score, showcasing the effectiveness of our approach in generating high-quality and semantically aligned images.

Method	Model Size	NFE	COCO FID ↓	HW FID ↓	COCO CLIP ↑
SDXL [11]	2.5B	32	14.28	7.96	31.68
SDXL-Turbo	2.5B	4	20.66	14.98	31.65
SDXL-Lightning [7]	2.5B	4	21.60	11.20	31.26
LCM [10]	0.86B	4	31.31	34.91	30.30
PixArt-δ [2]	0.6B	4	28.49	11.30	30.83
E2EDIFF	0.6B	4	25.27	9.76	32.76

4.2.1 Quantitative Results

To evaluate the effectiveness of our proposed method and compare it against state-of-the-art approaches, we conducted a comprehensive quantitative experiment. The quantitative comparison in Table 1 highlights the significant advantages of our method over state-of-the-art approaches across multiple evaluation metrics, demonstrating the effectiveness of our end-to-end training strategy. Unlike the compared methods, which rely on distillation techniques, our approach employs a small model trained entirely end-to-end, aligning the training process more closely with the sampling process and effectively bridging the gap between training and inference. In terms of image quality, as measured by FID, our method achieves superior performance on both COCO and HW datasets. The COCO FID underscores our model's ability to generate realistic images with fewer visual artifacts, while the HW FID demonstrates its capacity to produce aesthetically rich outputs. For text-image alignment, evaluated by CLIP score, our method achieves the highest score, reflecting stronger semantic consistency between the generated images and input prompts. This improvement can be attributed to the integration of LPIPS and GAN losses, which enhance both perceptual quality and semantic alignment. Moreover, despite having a significantly smaller model size and requiring only four sampling steps, our method surpasses larger models like SDXL in both image quality and alignment. These results validate the strength of our framework, which successfully balances high-quality generation, perceptual detail, and semantic accuracy, establishing itself as an efficient and scalable solution for text-to-image synthesis tasks.

4.2.2 Qualitative Results

To evaluate the effectiveness of our method in generating high-quality, aesthetically appealing, and semantically aligned images, we conducted a qualitative comparison with state-of-the-art approaches. Figure 2 presents the results across a variety of subjects, including human portraits and objects, in diverse styles. Our method demonstrates clear advantages in image quality, aesthetic appeal, and text-image alignment. The generated outputs exhibit finer details and sharper textures, such as individual hair strands, facial expressions, and material properties, resulting in more realistic and visually compelling images. Additionally, our approach consistently produces aesthetically superior outputs, particularly in stylized image generation tasks, where it effectively balances artistic style and content without sacrificing compositional harmony. In terms of semantic consistency, our method achieves stronger alignment between the generated images and input text prompts, benefiting from the integration of LPIPS and GAN losses, which enhance both perceptual fidelity and semantic relevance. These qualitative results, alongside quantitative findings, validate the effectiveness of our end-to-end training framework and loss function design, showcasing a robust balance between detail richness, aesthetic quality, and text-image alignment. This establishes our method as a versatile and efficient solution for diverse text-to-image synthesis tasks.

4.2.3 Ablation Study

Table 2. Ablation study of different loss combinations and their performance on text-to-image evaluation metrics. This experiment investigates the contribution of various loss components (L1, L2, LPIPS, and GAN) to the overall model performance. By selectively enabling or disabling these components, we analyze their impact on the image quality and text-image alignment of generated images. The results highlight how different loss combinations influence the final output, providing insights into the effectiveness of each component.

L1	L2	LPIPS	GAN	COCO FID ↓	HW FID ↓	COCO CLIP ↑
✓				25.61	10.15	31.32
	✓			25.34	9.91	31.31
		✓		26.68	10.11	31.24
	✓	✓		25.27	9.76	32.76
	✓	✓	✓	25.74	9.92	31.75

To investigate the impact of different loss functions on the performance of our model in text-to-image evaluation metrics, we specifically aim to understand the effects of incorporating perceptual loss (LPIPS) and GAN loss into the training process alongside baseline reconstruction losses such as L1 and L2. We hypothesize that combining multiple loss functions within our end-to-end training framework can lead to improved image quality, enhanced text-image align-

| SDXL-Turbo | SDXL-Light | LCM | PixelArt-δ | Ours |

Handsome man portrait, confident expression, soft lighting.

Lovely clothed panda, Cartoon, funny, Big Eyes, Cute, Oil Painting.

Chimney Rock State Park in North Carolina, Stock photography.

Raspberry fruit at 45-degree angle on pastel background, shadeless studio light, perspective shot, various forms.
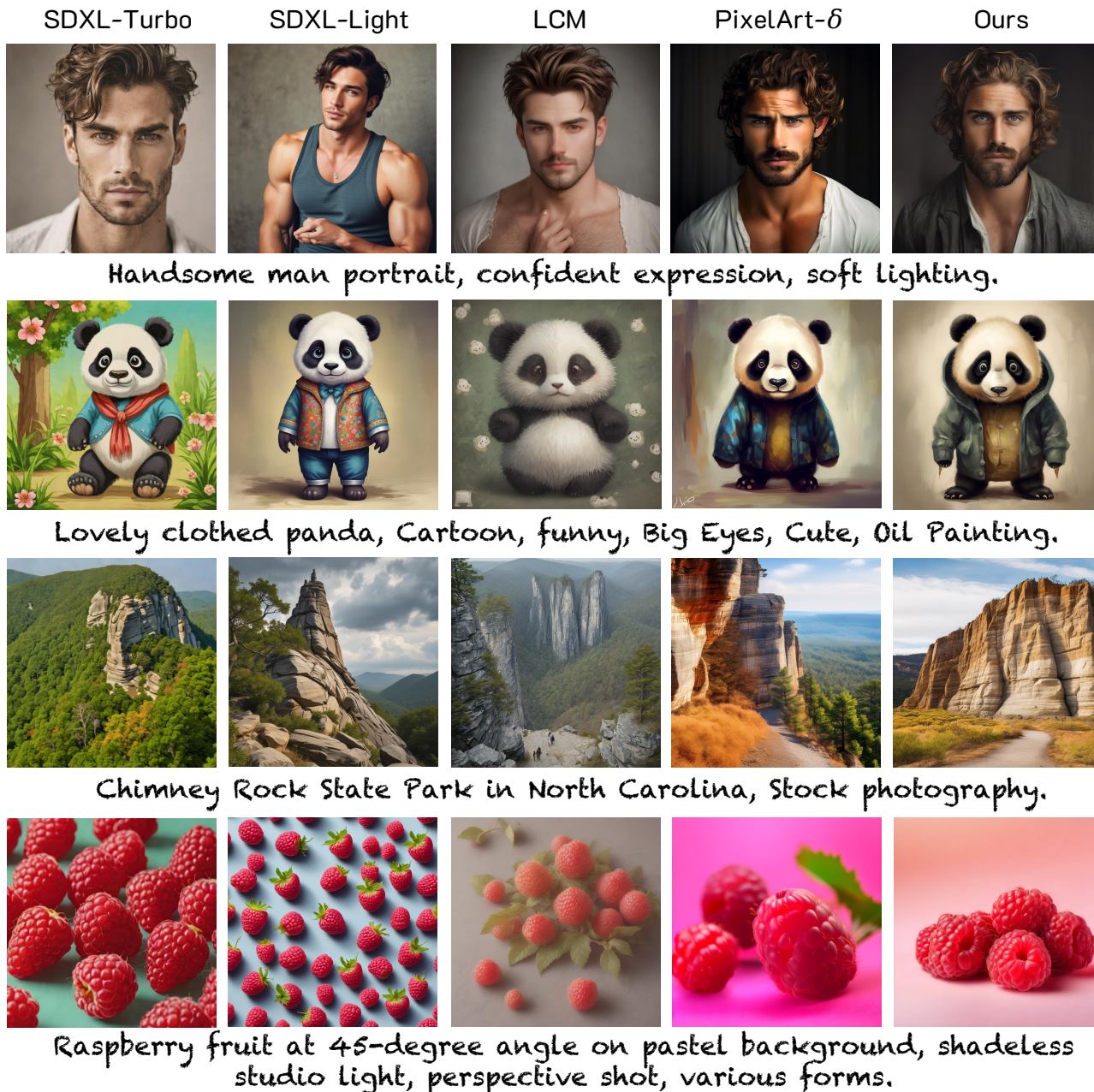
Figure 2. Visual comparison of image generation results across different methods on a variety of subjects (human portraits, objects) and styles. Our method demonstrates superior performance in terms of image quality, aesthetic appeal, and text-image alignment. The generated outputs exhibit finer details, richer textures, and better adherence to the input prompts compared to SOTA methods. This highlights the effectiveness of our end-to-end training framework and loss function design in balancing perceptual quality and semantic consistency.

ment, and greater perceptual realism compared to relying on single loss functions.

We conduct the ablation study using five distinct loss configurations. The first configuration uses L1 loss alone as a baseline, focusing on pixel-level reconstruction accuracy. The second replaces L1 with L2 loss, which offers a slightly different penalty for pixel-level discrepancies. The third configuration incorporates perceptual loss (LPIPS) to enhance the perceptual quality of generated images by considering feature-level similarities. The fourth combines LPIPS with L2 loss to balance perceptual quality and pixel-level fidelity. Finally, the fifth configuration integrates GAN loss alongside LPIPS and L2 losses, aiming to improve texture realism and introduce fine-grained details. To evaluate the

performance of these configurations, we measure COCO FID, HW FID, and COCO CLIP score on standard text-to-image benchmarks.

Quantitative Evaluation. The experimental results reveal several important insights into the impact of different loss functions on model performance. L2 loss demonstrates marginal advantages over L1 loss in pixel-level reconstruction, serving as a slightly more effective baseline. Incorporating LPIPS loss alone does not significantly improve performance but becomes highly effective when combined with L2 loss, resulting in enhanced perceptual quality and alignment across all metrics. Adding GAN loss to the combination of LPIPS and L2 introduces high-frequency details and textures, enriching the visual realism of generated images. However, this improvement comes with a slight trade-off in overall generation quality and text-image alignment. These observations highlight three key conclusions. First, our end-to-end training framework seamlessly integrates LPIPS and GAN losses, significantly improving image quality and text-image alignment. Second, while GAN loss enriches visual detail and texture, it introduces a trade-off between perceptual detail and metric performance. Lastly, combining multiple loss functions consistently outperforms single-loss configurations, demonstrating the value of leveraging complementary loss objectives. Together, these findings underscore the flexibility and effectiveness of our framework, providing a strong foundation for future advancements in generative modeling.

Qualitative Evaluation. To further analyze the effects of different loss functions, we present qualitative comparisons of the generated outputs for flowers and human portraits, as shown in Figure 3. The visualizations highlight the impact of GAN loss in generating high-frequency details. For example, in the generated human portraits, the inclusion of GAN loss results in finer details such as individual strands of hair, which significantly enhances the visual realism of the output. Similarly, in the flower images, the petal textures are noticeably richer and more detailed when GAN loss is used. These visual observations align with the quantitative results discussed earlier. While the addition of GAN loss slightly compromises overall FID and CLIP score, it introduces valuable perceptual details, enriching the generated images' realism. This trade-off underscores the complementary nature of combining LPIPS, L2, and GAN losses, which achieves a balance between perceptual detail and semantic alignment, as evident in both the quantitative and qualitative results. Together, these findings demonstrate the strength and flexibility of our end-to-end training framework for text-to-image generation tasks.

5. Conclusion

Diffusion models have established themselves as a leading framework for generative modeling, delivering state-

Figure 3. Qualitative comparison of generated results across different loss configurations. Each column represents a specific loss setting: L1, L2, LPIPS, L2+LPIPS, and L2+LPIPS+GAN. The inclusion of LPIPS loss improves perceptual quality, while combining L2+LPIPS with GAN loss adds high-frequency details, such as fine hair strands in portraits and intricate petal textures in flowers. Although this introduces a slight trade-off in text-image alignment, the combination of L2, LPIPS, and GAN losses achieves the best balance, producing realistic and semantically aligned outputs.

of-the-art performance across a variety of tasks. However, their potential is constrained by key limitations, including the training-sampling gap, information leakage in the noising process, and the inability to leverage advanced loss functions during training. In this work, we address these challenges through a novel end-to-end training framework that directly optimizes the full sampling trajectory. By aligning the training and sampling processes, our approach eliminates the training-sampling gap, mitigates information leakage by treating the training as a direct mapping from pure Gaussian noise to the target data distribution, and supports the incorporation of perceptual and adversarial losses to enhance image fidelity and semantic consistency. Our extensive experiments on COCO30K and HW30K benchmarks demonstrate the effectiveness of the proposed method, achieving superior performance in terms of Fréchet Inception Distance (FID) and CLIP score. These results underscore the robustness and efficiency of the end-to-end training paradigm, paving the way for advancing diffusion-based generative models toward more practical and high-quality solutions. Future work will explore extending this framework to other generative tasks and further optimizing the computational efficiency of the approach.

References

[1] Nicholas Carlini, Matthew Jagielski, Christopher A Choquette-Choo, Daniel Paleka, Will Pearce, Hyrum Anderson, Andreas Terzis, Kurt Thomas, and Florian Tramèr. Poisoning web-scale training datasets is practical. In *2024 IEEE Symposium on Security and Privacy (SP)*, pages 407–425. IEEE, 2024.

[2] Junsong Chen, Yue Wu, Simian Luo, Enze Xie, Sayak Paul, Ping Luo, Hang Zhao, and Zhenguo Li. Pixart-{\delta}: Fast and controllable image generation with latent consistency models. *arXiv preprint arXiv:2401.05252*, 2024.

[3] Ian Goodfellow, Jean Pouget-Abadie, Mehdi Mirza, Bing Xu, David Warde-Farley, Sherjil Ozair, Aaron Courville, and Yoshua Bengio. Generative adversarial networks. *Communications of the ACM*, 63(11):139–144, 2020.

[4] Martin Heusel, Hubert Ramsauer, Thomas Unterthiner, Bernhard Nessler, and Sepp Hochreiter. Gans trained by a two time-scale update rule converge to a local nash equilibrium. *Advances in neural information processing systems*, 30, 2017.

[5] Jonathan Ho, Ajay Jain, and Pieter Abbeel. Denoising diffusion probabilistic models. *Advances in neural information processing systems*, 33:6840–6851, 2020.

[6] Diederik P Kingma. Auto-encoding variational bayes. *arXiv preprint arXiv:1312.6114*, 2013.

[7] Shanchuan Lin, Anran Wang, and Xiao Yang. Sdxl-lightning: Progressive adversarial diffusion distillation. *arXiv preprint arXiv:2402.13929*, 2024.

[8] Tsung-Yi Lin, Michael Maire, Serge Belongie, James Hays, Pietro Perona, Deva Ramanan, Piotr Dollár, and C Lawrence Zitnick. Microsoft coco: Common objects in context. In *Computer Vision–ECCV 2014: 13th European Conference, Zurich, Switzerland, September 6-12, 2014, Proceedings, Part V 13*, pages 740–755. Springer, 2014.

[9] Haotian Liu, Chunyuan Li, Qingyang Wu, and Yong Jae Lee. Visual instruction tuning. *Advances in neural information processing systems*, 36, 2024.

[10] Simian Luo, Yiqin Tan, Longbo Huang, Jian Li, and Hang Zhao. Latent consistency models: Synthesizing high-resolution images with few-step inference. *arXiv preprint arXiv:2310.04378*, 2023.

[11] Dustin Podell, Zion English, Kyle Lacey, Andreas Blattmann, Tim Dockhorn, Jonas Müller, Joe Penna, and Robin Rombach. Sdxl: Improving latent diffusion models for high-resolution image synthesis. *arXiv preprint arXiv:2307.01952*, 2023.

[12] Alec Radford, Jong Wook Kim, Chris Hallacy, Aditya Ramesh, Gabriel Goh, Sandhini Agarwal, Girish Sastry, Amanda Askell, Pamela Mishkin, Jack Clark, et al. Learning transferable visual models from natural language supervision. In *International conference on machine learning*, pages 8748–8763. PMLR, 2021.

[13] Robin Rombach, Andreas Blattmann, Dominik Lorenz, Patrick Esser, and Björn Ommer. High-resolution image synthesis with latent diffusion models. In *Proceedings of the IEEE/CVF conference on computer vision and pattern recognition*, pages 10684–10695, 2022.

[14] Tim Salimans and Jonathan Ho. Progressive distillation for fast sampling of diffusion models. *arXiv preprint arXiv:2202.00512*, 2022.

[15] Jiaming Song, Chenlin Meng, and Stefano Ermon. Denoising diffusion implicit models. In *International Conference on Learning Representations*, 2021.

[16] Yang Song and Prafulla Dhariwal. Improved techniques for training consistency models. *arXiv preprint arXiv:2310.14189*, 2023.

[17] Yang Song, Prafulla Dhariwal, Mark Chen, and Ilya Sutskever. Consistency models. *arXiv preprint arXiv:2303.01469*, 2023.

[18] Yang Song, Jascha Sohl-Dickstein, Diederik P Kingma, Abhishek Kumar, Stefano Ermon, and Ben Poole. Score-based generative modeling through stochastic differential equations. *arXiv preprint arXiv:2011.13456*, 2020.